Quantitative and anisotropic mechanochromism of polydiacetylene at nanoscale

Levente Juhasz[1§], Roberto D. Ortuso[1,3§], Kaori Sugihara[2,1*]

ABSTRACT: Quantitative and anisotropic mechanochromism of polydiacetylene over nanoscale distances remains unaddressed even after 50 years of extensive research. This is because its anisotropic structure on substrates necessitates the application of both vertical and lateral forces (shear forces) to characterize it, whereas atomic force microscopy, which is the usual technique used to investigate nanoscale forces, is only capable of quantifying vertical forces. In this study, we address this lacuna by utilizing quantitative friction force microscopy that measures lateral forces. Our data confirm that polydiacetylene reacts only to lateral forces, $F_{//}$, and disprove the previously-claimed hypothesis that the edges of the polymer crystals exhibit higher force sensitivity than the rest of the crystal. In addition, we report a correlation between mechanochromism and thermochromism, which can be attributed to the fact that both work and heat are different means of providing the same transition energy.

KEYWORDS: Polydiacetylene, Langmuir-Blodgett films, atomic force microscopy, quantitative friction force microscopy, fluorescence microscopy

Polydiacetylene (PDA) is a class of mechanochromic polymers, including non-amphiphilic and amphiphilic ones with hydrophobic (*e.g.* alkyl[1], aryl[2]) chains on one end, and a hydrophilic headgroup (*e.g.* -COOH[3], -NH_2[4], -ester[5]) or other moieties (*e.g.* aryl[6, 7]-, etoxisilane[8]-, urethane[7]-, isocyanate[9]-groups) on the other end, that was initially reported in the late 1960s.[10] It is known to change color and become fluorescent when it is exposed to heat,[11] pH variation,[12] adsorption of ions[13], and other molecules.[14, 15] Over the years, its monomer assembly, polymerization process, polymer structure, and mechanochromic properties have been characterized based on measurements via the Langmuir-Blodgett technique,[16] electron paramagnetic resonance (EPR),[17] X-ray crystallography,[18] UV-VIS,[19] fluorescence,[20] infrared (IR),[21] Raman spectroscopy,[22] nuclear magnetic resonance (NMR),[23] scanning tunneling microscopy (STM),[24] atomic force microscopy (AFM),[25] fluorescence microscopy[26] and electrical conductivity.[27] The experimental results, together with theoretical works[28], have provided a mechanistic model of PDA, which identifies the torsion in its backbone to be the origin of its force sensitivity, although a lack of separation between the single-polymer and the aggregate-induced effects makes it difficult to clarify its intrinsic properties. However, despite extensive research, the most fundamental characteristic of PDA mechanochromism — the variation of its optical properties as a function of quantitative and anisotropic external forces at nanoscale — has not been investigated. Certain studies have utilized macroscopic and microscopic stretch,[25, 29] macroscopic scratching,[30] tuned oscillatory devices,[31] compression using the Langmuir–Blodgett trough,[32] and rheometers[33], in addition to other qualitative methods such as grinding[34], to characterize PDA mechanochromism. AFM studies, which measure the correlation between applied forces and the induced fluorescence in PDA,[25, 35] have provided the most detailed insights into PDA mechanochromism over nanoscale distances. Burns et al. concluded that the application of lateral forces on the substrate (shear forces) is essential to activate PDA fluorescence[25]. Recently, Polacchi *et al.* reported the quantitative correlation between PDA fluorescence and applied forces.[35] Although these works provided preliminary accounts of PDA mechanochromism over nanoscale distances, they quantitatively studied only vertical forces, and treated the more important lateral forces qualitatively. This is primarily because

standard AFM cannot be used to quantify forces parallel to the substrate. This hinders the quantitative study of anisotropic PDA mechanochromism.

In this study, we couple quantitative friction force microscopy, which enables lateral force quantification, with fluorescence microscopy (Figure 1a) to quantitatively investigate the anisotropic mechanochromism of PDA over nanoscale distances. The utilization of this experimental technique was partially enabled by our recent identification of an error source in quantitative friction force microscopy over the nanonewton range.[36] Using this setup, we answer the following open questions in the field — is PDA mechanochromism truly anisotropic? Is force sensitivity at the edges of the crystals different from that in their bulk? Is there a correlation between thermochromism and mechanochromism?

Fabrication of PDA films. PDAs were deposited on glass coverslips by the vertical transfer of diacetylene monomers via the Langmuir–Blodgett method, followed by UV crosslinking. These samples were placed on an inverted fluorescence microscope coupled with a quantitative friction force microscope. The quantitative friction force microscopy was calibrated using the wedge calibration method developed by Ogletree et al.[37] and improved by Varenberg et al.[38] Previously, we had experienced an amplification of errors when this wedge calibration method was applied at nanonewton force ranges. However, we had identified the origin of the error and had provided a method to avoid this inaccuracy.[36] We used the hover mode, in which the AFM tip remains in contact with the sample only on the way (trace) and hovers over it on the way back (re-trace), avoiding contact with the surface. This enables the unidirectional application of lateral forces to the PDA sample only once corresponding to each scanning line, thereby avoiding complications in the interpretation of the obtained data.

The mechanochromism of PDA was observed to be anisotropic over nanoscale distances. PDA comprising 5,7-docosadiynoic acid (DCDA) induced the formation of micro-sized crystals with an average height of 12.81 ± 1.26 nm on the glass coverslips, as observed via bright field microscopy (Figure 1b) and

AFM topology (Figure 1c). These substrates were scanned by AFM at setpoints (vertical forces) of 20, 40, 60, 80, and 100 nN (Figure 1f). Fluorescence images were captured before and after scanning, and their difference (Δ fluorescence) was quantified (Figure 1d). During the scanning, the AFM cantilever was also used to apply lateral forces to the PDA, as quantified by the tilt of the tip and the consequent lateral deflection of the laser. Quantitative friction force microscopy enabled the measurement of this lateral force applied by the tip to the sample at each location, enabling the construction of a complete lateral force map, as depicted in Figure 1e. A comparison between the Δ fluorescence, $F_{//}$, and $F_{\perp}$ maps confirmed that Δ fluorescence is correlated with the lateral forces, $F_{//}$, rather than the vertical ones, $F_{\perp}$ (Figure 1d-f). This suggests that PDA reacts only to shear forces, as it has been proposed before[25].To further compare the spatial maps of height, Δ fluorescence, lateral force, and vertical force over nanoscale distances, expanded images of the white squares indicated in Figure 1c-f and the cross sections of PDA crystals inside them are depicted in Figure 1g. At the edges of the PDA crystals, where the AFM tip entered the object, the lateral force was observed to increase by 253 % compared to that in the glass areas (consult the cross sections depicted in Figure 1g). In the inner part of the PDA crystal, the measured lateral force was similar to that on the glass (consult the cross sections depicted in Figure 1g corresponding to 1 μm < distance < 1.5 μm). The friction between the tip and the PDA was frequently observed to be equal to or lower than that between the tip and the glass, as is evident from the contrast in Figure 1e. The crystal edges on which high lateral force was applied, exhibited high fluorescence intensity, as evidenced by the co-localization of high lateral forces and high fluorescence intensity variations under constant vertical forces (Figure 1g). This provides further evidence for the fact that the fluorescence in PDA is correlated with the lateral forces, rather than the vertical ones, over nanoscale distances, even within a single crystal. Previously, a quantitative link between Δ fluorescence and the vertical force, $F_{\perp}$, had been reported.[35] However, the spatial correlation between Δ fluorescence and the vertical force, $F_{\perp}$, over nanoscale distances is observed to be insignificant in the data obtained in this study.

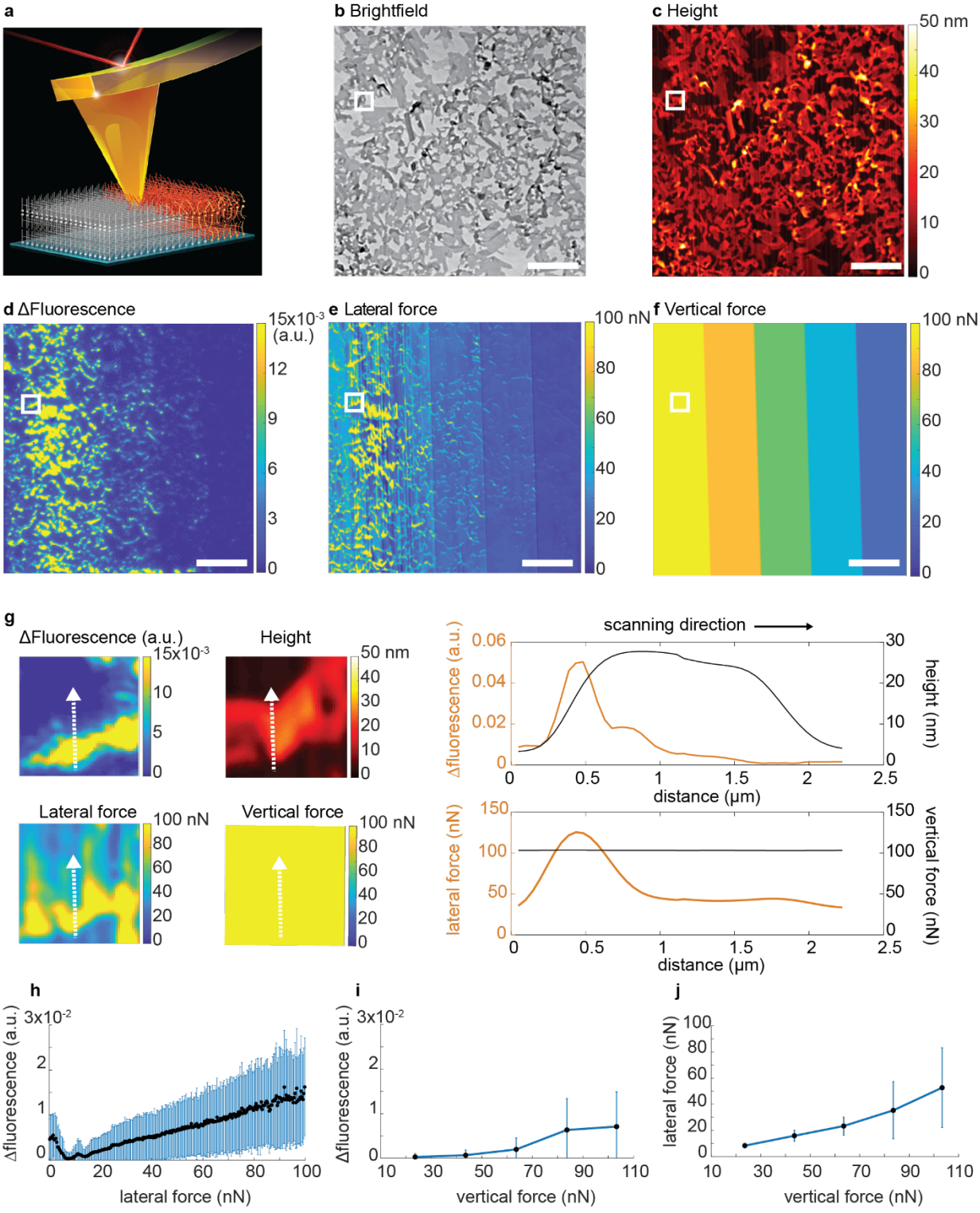

Figure 1. Characterization of 5,7-docosadiynoic acid (DCDA) Langmuir-Blodgett films by lateral force microscopy coupled with fluorescence microscopy. **a**, A scheme of the experiment. **b**, Brightfield microscopy image. **c**, AFM height image. **d**,

Fluorescence increase map. **e**, Lateral force map. **f**, Vertical force map. The scale bars show 10 μm. **g**, Zoom-in images of the white squares in images (c-f) and cross-sections along the white dotted arrows. Note that the white arrows in the zoom-in images showing the scanning direction are slightly tilted due to the alignment of the AFM images to optical images. These Δ fluorescence, Lateral force, Vertical force maps were correlated pixel by pixel and binned to generate plots in h-j; **h**, Fluorescence increase vs. lateral force, **i**, Fluorescence increase vs. vertical force, **j**, Lateral force as a function of the applied vertical force. The error bars show the standard deviation in each bin. Lateral force microscopy experiments were carried out in contact hover mode, with increasing setpoints (i.e. vertical force) after each 100 lines (20, 40, 60, 80 and 100 nN) at 4 μm/s scanning speed. Areas of 50 x 50 μm were scanned at a resolution of 512 x 512 pixel.

Fluorescence was observed to be directly proportional to lateral forces, whereas it exhibited a pseudo-correlation with vertical forces because the lateral and vertical forces are related by the friction law.

To ascertain the origin of this unintuitive correlation between Δ fluorescence and $F_{\perp}$, we plotted the values of Δ fluorescence against those of $F_{//}$ and $F_{\perp}$ in Figure 1d-f in a pixel-by-pixel manner. This analysis required a series of procedures, including the removal of the glass region by identifying the PDA location via thresholding, binarization, and spatial superposition of fluorescence images and force maps (consult Materials and Methods for further details). As expected, Δ fluorescence was observed to be directly proportional to the lateral force, $F_{//}$, with a slope coefficient of 1.19×10^{-4} nN^{-1} (Figure 1h). Despite no obvious spatial colocalization of their intensity profiles, Δ fluorescence and $F_{\perp}$ were also observed to be correlated with a slope coefficient of 0.97×10^{-4} nN^{-1} (Figure 1i). This is because Δ fluorescence is proportional to the lateral force, $F_{//}$, and the average lateral force, $F_{//}$, and the vertical force, $F_{\perp}$, are related via the friction law, $F_{//} = \mu F_{\perp}$ (Figure 1j). Lateral force has a general propensity of displaying a higher value as vertical forces increase. This can be explained by the classic friction law, $F_{//} = \mu F_{\perp}$, where the friction force $F_{//}$ is proportional to the weight of the object ($F_{\perp}$: vertical force) with a friction coefficient μ. As a result, when Δ fluorescence vs $F_{\perp}$ has a linear relationship, Δ fluorescence vs $F_{//}$ will also have a linear relationship because of $F_{//} = \mu F_{\perp}$. The slope coefficient of the $F_{//}$ vs $F_{\perp}$ plot in Figure 1j was 0.54, which is larger than the measured friction coefficient between the tip and the inner bulk of the PDA crystals (0.34).

This can be attributed to the elevation of the average lateral forces by the high lateral force exhibited at the edge of the crystals upon impact of the tip, which does not obey the classic friction law. The obtained data demonstrated that the reason why Δ fluorescence appears to be proportional to $F_{\perp}$ despite the fact that PDA reacts only against $F_{//}$ is because $F_{\perp}$ and $F_{//}$ are linked via the friction law.

The sensitivity of mechanochromism at the edges of PDA crystals was observed to be identical to that within their bulk. As mentioned previously, the edges of PDA crystals were typically observed to exhibit high Δ fluorescence, which had also been reported by previous studies[20, 25]. As the magnitude of the vertical force, $F_{\perp}$ (setpoint), was kept constant during the scanning process, it had been hypothesized in previous studies that the crystal edges exhibit higher force sensitivity compared to their inner bulk due to the structural differences between them, where the larger amount of free space at the edges facilitates the torsions in the backbone. Although this idea seemed reasonable, the data obtained in this study disproved this hypothesis. First, we separated each Δ fluorescence, $F_{//}$, and $F_{\perp}$ map into portions corresponding to the inner bulk of crystals and their edges (Figure 2a-c). The signals from the glass regions were removed from these images to highlight the structure of the PDA crystals. The edges of the PDA islands were defined to be the 3 outermost pixels (145 nm). A thickness of 3 pixels was chosen to select the high Δ fluorescence area without including too much of the inner bulk with lower fluorescence intensity. Due to this policy of underselection, the "inner part" contained a small fraction of high-Δ fluorescence regions. These separated images were correlated pixel-by-pixel to individually visualize Δ fluorescence vs $F_{//}$ at the edges and the inner portions of the crystals. Δ fluorescence vs $F_{//}$ plots depicted no significant difference between the two scenarios (Figure 2d), establishing that the PDA sensitivity is independent of inner or edge structure of the PDA crystals. The same conclusion was obtained by using PDAs comprising two other diacetylene monomers (Figure S2d, S4d), confirming this to be a general result. The expectation that crystal edges exhibit higher force sensitivity arose from the wrong premise that PDA reacts to $F_{\perp}$, which has already been disproved by this study, as depicted in Figure 1. The comparison of Δ fluorescence with $F_{//}$, which is

the real parameter that governs PDA mechanochromism, reveals no sensitivity difference between the edges and the inner parts of PDA crystals.

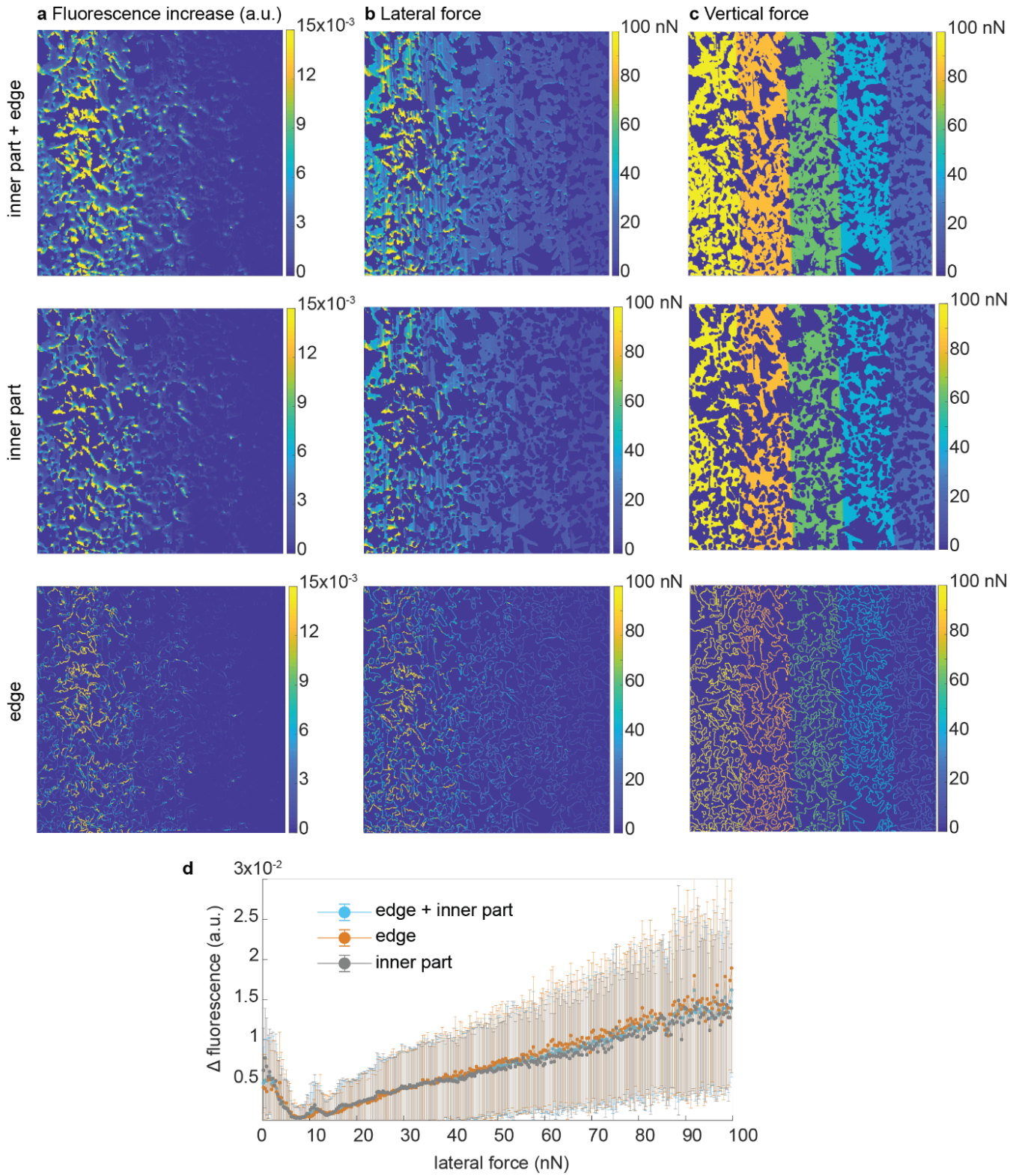

Figure 2. Separation of the inner part and edge of the PDA islands in lateral force microscopy experiments. **a**, Fluorescence increase of DCDA LB films, **b**, lateral force map and **c**, vertical force map. The images in the upper row show the whole scanned region without separation, the middle row shows only the inner parts of the PDA islands, while the edge regions of the PDA islands are displayed in the bottom row. The edge of a PDA island is defined as the 3 outermost pixels (145 nm). Note, that the images are slightly tilted due to the alignment of AFM to optical data. **d**, Fluorescence increase as a function of lateral force after binning, separated for the inner part and edge regions. The error bars show the standard deviation in each bin.

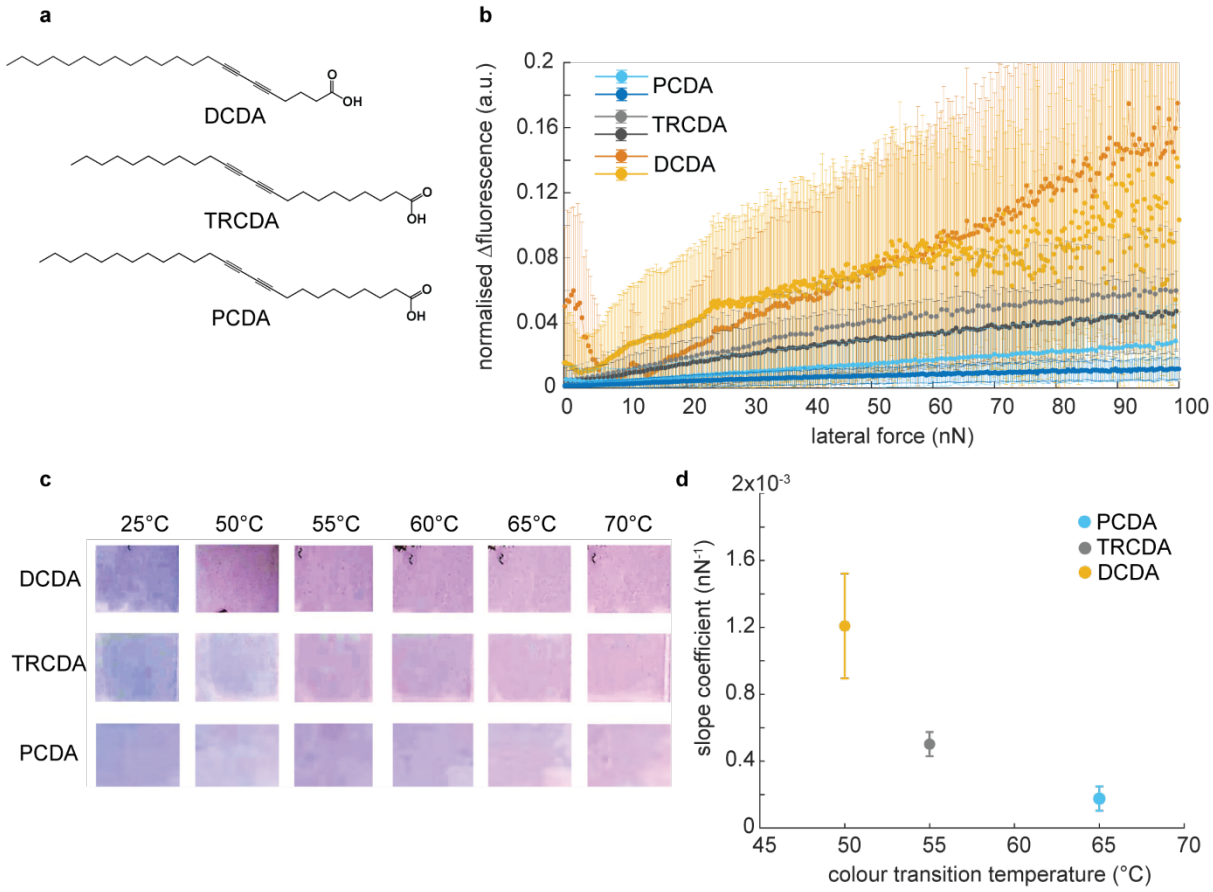

Figure 3. PDA force sensitivity depends on its thermochromic temperature. **a**, Structures of the studied diacetylene monomers. **b**, Normalized fluorescence increase as a function of lateral force for 10,12-pentacosadiynoic acid (PCDA), 10,12-tricosadiynoic acid (TRCDA) and 5,7-docosadiynoic acid (DCDA). Two samples were studied for each PDA. The error bars show the standard deviation in each bin. **c**, Photographs taken of DCDA, TRCDA and PCDA LB films on glass coverslips during heating on a hot plate. (Due to the reversible thermochromism of DCDA at lower temperatures[39], colour monitoring had to be performed in situ.) **d**, Average slope coefficients from two samples for each PDA. Extracted from (b) by linear fitting as a function of the thermochromic transition temperature for PCDA, TRCDA and DCDA after binning.

PDA with lower thermochromic transition temperatures exhibited higher force sensitivity. To investigate the relationship between thermochromism and mechanochromism, we repeated the experiment with PDAs comprising 10,12-tricosadiynoic acid (TRCDA) and 10,12-pentacosadiynoic acid (PCDA), which possess the same carboxyl headgroup as DCDA, but exhibit higher thermochromic temperatures due to the difference between the carbon chain numbers or the location of the triple bond (Figure 3a). The results corresponding to PCDA and TRCDA were observed to be qualitatively similar to those in the case of DCDA (Figure S1-S3). However, quantitatively, the slope coefficients of the Δ fluorescence with respect to $F_{//}$ were observed to be unique for each PDA (Figure 3b. Δ fluorescence was normalized using the maximum fluorescence observed after the heat treatment, which enabled the quantification of the fraction of PDA activated by the forces.[40] Consult Materials and Methods for further details)—DCDA ((1.2 ± 0.3) x 10^{-3} nN^{-1}) > TRCDA ((5.0± 0.7) x 10^{-4} nN^{-1}) > PCDA ((1.8± 0.7) x $10^{-4}$$nN^{-1}$). This was the opposite of the order with respect to the thermochromic temperatures: PCDA (65 °C) > TRCDA (55 °C) > DCDA (50 °C) (Fig. 3c-d). This suggested that PDAs with lower thermochromic temperatures exhibit higher force sensitivities. A similar trend has been previously observed by Terada and coworkers[41], where PDA-organic amine composites were characterized by applying macroscopic friction forces with a cage. There has been a hypothesis that the motion of the left-over monomers in PDAs are facilitating the color change especially in case of peptide-induced chromism[42], whereas it has been rejected for the thermochromism[43]. In our case, the amount of the left-over monomers is estimated to be in the order of TRCDA > PCDA > DCDA based on the fluorescence intensity after the complete activation by heat, whereas the force sensitivity was in the order of DCDA > TRCDA > PCDA. Therefore, we did not see a direct correlation in the present case.

Previously, X-ray crystallography[44], nuclear magnetic resonance (NMR)[23], infrared (IR)[21] and Raman spectroscopy[45] had been used to detect increase in structural disorder during blue-to-red transition. This indicates that PDA chromism is often associated with the crystal-to-amorphous transition. To crush nicely aligned PDAs into an amorphous state, hydrogen bonds in the headgroups and hydrophobic interactions in their tails need to be broken. The breaking of hydrogen bonds requires approximately 6-30 kJ/mol[46, 47] and

the dissociation of hydrophobic attractions between molecules requires approximately 10 kJ/mol/nm^2,[48] in contrast to the breaking of covalent bonds, which typically requires hundreds of kJ/mol. In the case of thermochromism, these energies are provided by heat. In the case of mechanochromism, they are provided by work, $W = F\Delta x$. This explains the correlation between force sensitivity and the thermochromic temperature, as both work and heat are different means of providing the same transition energy. Our experiment measured this force to be in a nanonewton range. This can be rationalized as follows. Translating the work into forces requires a length scale, until the binding forces hold. For example, for hydrogen bonds and hydrophobic attractions, which persist over distances of ~ 1 nm, the force required to break a bond is of an order of magnitude of ~ 17 pN (= 10 kJ/6.02 x 10^{23}/1 nm), in contrast to covalent bonds that require ~ 1.7 nN (= 100 kJ/6.02 x 10^{23}/0.1 nm; covalent bonds persist over a smaller distance of ~ 0.1 nm).[49] Considering that the AFM tip used in this study had a tip radius of 35 nm, the tip-PDA contact involved the simultaneous severance of hundreds of bonds (17 pN× 100 = 1.7 nN). Therefore, the expected force required to crush PDA crystals into an amorphous state is in a nanonewton range, which does not contradict with our experimental results. However, the accurate force calculation requires the expression of the potential profile as a function of distance. The reason why the same amount of vertical forces did not activate the PDA also reflects that the translation of energy into forces is more complex. These arguments are approximation as the energy barrier between the blue and red states that has been previously estimated by thermochromism (~84 kJ/mol = ~20 kcal/mol)[39, 50, 51] is slightly higher than the energy required to simply break the bonds (6-30 kJ/mol[46, 47]). This implies that the system requires an additional energy penalty to non-planarize the conjugated backbone in addition to breaking the bonds to cause thermochromism. Once the system is pushed over the potential wall between the blue and red states, entropy decreases the final energy of the red state and makes it stable, as many PDAs are nonreversible.

Conclusions

We reported a quantitative evaluation of anisotropic mechanochromism of polydiacetylene over nanoscale distances by utilizing quantitative friction force microscopy, which enabled the measurement of lateral forces. We found that PDA reacts only against lateral forces, $F_{//}$. On the other hand, the previously reported relationship between vertical forces $F_{\perp}$ and Δ fluorescence was confirmed to be a pseudo-correlation propagated via the friction law ($F_{//} = \mu F_{\perp}$). Further, the hypothesis that the edges of the PDA crystals exhibit higher force sensitivity was disproved by the measurements of this study, as the Δ fluorescence-$F_{//}$ curve exhibited no significant difference corresponding to the edges and the inner bulks of the crystals. We also found that PDA crystals with lower thermochromic temperatures exhibit higher force sensitivity, which can be attributed to the fact that both work and heat are sources of transition energy. The presented local force response of PDA probably mainly reflects the aggregate-induced mechanochromic behavior, as disturbing the alignment of the crystal by friction force microscopy turned on the fluorescence, although the effect of the associated structural change of a single polymer is also not excluded as they are difficult to separate. After decades of efforts to study the behavior of PDA chromism with respect to variations in heat, pH change, ions, peptides, etc., the presented quantitative and anisotropic mechanochromism at nanoscale will finally expedite the utilization of PDA as a unique nano-force sensor that detects forces by twist in contrast to other mechanophores [52, 53] in future. In addition, the combined friction force and fluorescence microscopy setup used in the present work can be used as a general method to extract quantitative and anisotropic force responses at nanoscale in other mechanochromic materials.

Acknowledgements

Part of the research leading to these results has received funding from Swiss National Foundation, the Swiss National Centre of Competence in Research (NCCR) Chemical Biology, Fondation Ernst et Lucie Schmidheiny, Leading House for the Middle East and North Africa (University of Applied Sciences and Arts Western Switzerland), FY 2020 University of Tokyo Excellent Young Researcher, the Female Faculty

Startup Grant, the special fund of Institute of Industrial Science, the University of Tokyo, JSPS KAKENHI Grant Number JP20K22324, the Naito Foundation and Kanamori Foundation. We thank Jiangtao Zhao and Johann Nuck for fruitful discussions during the project.

Author information

[1]Department of Physical Chemistry, University of Geneva, Quai Ernest Ansermet 30, 1211 Geneva 4, Switzerland

[2]Institute of Industrial Science, The University of Tokyo, 4-6-1 Komaba Meguro-Ku, Tokyo 153-8505, Japan

[3]Adolphe Merkle Institute, University of Fribourg, Chemin des Verdiers 4, 1700 Fribourg, Switzerland

[§]equal contribution

*corresponding author: kaori-s@iis.u-tokyo.ac.jp

Supporting information

Supporting figures (Figure S1 – S4) and Materials and Method are provided in Supplementary Information.

References

1. Okada S, Peng S, Spevak W, Charych D. Color and chromism of polydiacetylene vesicles. *Accounts Chem Res* 1998, **31**(5)**:** 229-239.

2. Ikeshima M, Katagiri H, Fujiwara W, Tokito S, Okada S. Synthesis, Crystal Structures, and Solid-State Polymerization of 8-[4-(Dimethylamino)phenyl]octa-5,7-diynyl Carbamates. *Crystal Growth & Design* 2018, **18**(10)**:** 5991-6000.

3. Carpick RW, Sasaki DY, Marcus MS, Eriksson MA, Burns AR. Polydiacetylene films: a review of recent investigations into chromogenic transitions and nanomechanical properties. *Journal of Physics: Condensed Matter* 2004, **16**(23)**:** R679-R697.

4. Seo D, Kim J. Effect of the Molecular Size of Analytes on Polydiacetylene Chromism. *Adv Funct Mater* 2010, **20**(9)**:** 1397-1403.

5. Park IS, Park HJ, Jeong W, Nam J, Kang Y, Shin K, Chung H, Kim J-M. Low Temperature Thermochromic Polydiacetylenes: Design, Colorimetric Properties, and Nanofiber Formation. *Macromolecules* 2016, **49**(4)**:** 1270-1278.

6. Sarkar A, Okada S, Matsuzawa H, Matsuda H, Nakanishi H. Novel polydiacetylenes for optical materials: beyond the conventional polydiacetylenes. *J Mater Chem* 2000, **10**(4)**:** 819-828.

7. Lee DC, Sahoo SK, Cholli AL, Sandman DJ. Structural aspects of the thermochromic transition in urethane-substituted polydiacetylenes. *Macromolecules* 2002, **35**(11)**:** 4347-4355.

8. Ahn DJ, Lee S, Kim JM. Rational Design of Conjugated Polymer Supramolecules with Tunable Colorimetric Responses. *Adv Funct Mater* 2009, **19**(10)**:** 1483-1496.

9. Park IS, Park HJ, Kim JM. A soluble, low-temperature thermochromic and chemically reactive polydiacetylene. *ACS Appl Mater Interfaces* 2013, **5**(17)**:** 8805-8812.

10. Gerhard, W. Journal of Polymer Science Part B: Polymer Letters 1971, 9, (2), 133-144.

11. Girard-Reydet C, Ortuso RD, Tsemperouli M, Sugihara K. Combined Electrical and Optical Characterization of Polydiacetylene. *Journal of Physical Chemistry B* 2016, **120**(14)**:** 3511-3515.

12. Kew SJ, Hall EAH. pH response of carboxy-terminated colorimetric polydiacetylene vesicles. *Anal Chem* 2006, **78**(7)**:** 2231-2238.

13. Xu Q, Lee S, Cho Y, Kim MH, Bouffard J, Yoon J. Polydiacetylene-Based Colorimetric and Fluorescent Chemosensor for the Detection of Carbon Dioxide. *J Am Chem Soc* 2013, **135**(47)**:** 17751-17754.

14. Ortuso RD, Cataldi U, Sugihara K. Mechanosensitivity of polydiacetylene with a phosphocholine headgroup. *Soft Matter* 2017, **13**(8)**:** 1728-1736.

15. Kolusheva S, Boyer L, Jelinek R. A colorimetric assay for rapid screening of antimicrobial peptides. *Nat Biotechnol* 2000, **18**(2)**:** 225-227.

16. Lifshitz Y, Upcher A, Shusterman O, Horovitz B, Berman A, Golan Y. Phase transition kinetics in Langmuir and spin-coated polydiacetylene films. *Phys Chem Chem Phys* 2010, **12**(3)**:** 713-722.

17. Sixl H, Neumann W, Huber R, Denner V, Sigmund E. Electron-Spin-Resonance Experiments and Theory of the Butatriene-to-Acetylene Transition in Short-Chain Polydiacetylene Molecules. *Phys Rev B* 1985, **31**(1)**:** 142-148.

18. Lifshitz Y, Golan Y, Konovalov O, Berman A. Structural Transitions in Polydiacetylene Langmuir Films. *Langmuir* 2009, **25**(8)**:** 4469-4477.

19. Chance RR, Patel GN. Solid-State Polymerization of a Diacetylene Crystal - Thermal, Ultraviolet, and Gamma-Ray Polymerization of 2,4-Hexadiyne-1,6-Diol Bis-(Para-Toluene Sulfonate). *J Polym Sci Pol Phys* 1978, **16**(5)**:** 859-881.

20. Carpick RW, Sasaki DY, Burns AR. First observation of mechanochromism at the nanometer scale. *Langmuir* 2000, **16**(3)**:** 1270-1278.

21. Ortuso RD, Ricardi N, Burgi T, Wesolowski TA, Sugihara K. The deconvolution analysis of ATR-FTIR spectra of diacetylene during UV exposure. *Spectrochim Acta A Mol Biomol Spectrosc* 2019, **219:** 23-32.

22. Yager P, Schoen PE, Davies C, Price R, Singh A. Structure of lipid tubules formed from a polymerizable lecithin. *Biophys J* 1985, **48**(6)**:** 899-906.

23. Jelinek R, Okada S, Norvez S, Charych D. Interfacial catalysis by phospholipases at conjugated lipid vesicles: colorimetric detection and NMR spectroscopy. *Chemistry & Biology* 1998, **5**(11)**:** 619-629.

24. Okawa Y, Aono M. Nanoscale control of chain polymerization. *Nature* 2001, **409**(6821)**:** 683-684.

25. Burns AR, Carpick RW, Sasaki DY, Shelnutt JA, Haddad R. Shear-induced mechanochromism in polydiacetylene monolayers. *Tribol Lett* 2001, **10**(1-2)**:** 89-96.

26. Dubin F, Melet R, Barisien T, Grousson R, Legrand L, Schott M, Voliotis V. Macroscopic coherence of a single exciton state in an organic quantum wire. *Nat Phys* 2006, **2**(1)**:** 32-35.

27. Okawa Y, Aono M. Nanoscale wiring by controlled chain polymerization. *Surface Science* 2002, **514**(1-3)**:** 41-47.

28. Dobrosavljevic V, Stratt RM. Role of Conformational Disorder in the Electronic-Structure of Conjugated Polymers - Substituted Polydiacetylenes. *Phys Rev B* 1987, **35**(6)**:** 2781-2794.

29. Nallicheri RA, Rubner MF. Investigations of the Mechanochromic Behavior of Poly(Urethane Diacetylene) Segmented Copolymers. *Macromolecules* 1991, **24**(2)**:** 517-525.

30. Terada H, Imai H, Oaki Y. Visualization and Quantitative Detection of Friction Force by Self-Organized Organic Layered Composites. *Adv Mater* 2018, **30**(27).

31. Feng HB, Lu J, Li JH, Tsow F, Forzani E, Tao NJ. Hybrid Mechanoresponsive Polymer Wires Under Force Activation. *Adv Mater* 2013, **25**(12)**:** 1729-1733.

32. Sasaki DY, Carpick RW, Burns AR. High molecular orientation in mono- and trilayer polydiacetylene films imaged by atomic force microscopy. *J Colloid Interface Sci* 2000, **229**(2)**:** 490-496.

33. Lee SS, Chae EH, Ahn DJ, Ahn KH, Yeo JK. Shear-induced color transition of PDA (polydiacetylene) liposome in polymeric solutions. *Korea-Aust Rheol J* 2007, **19**(1)**:** 43-47.

34. Ishijima Y, Imai H, Oaki Y. Tunable Mechano-responsive Color-Change Properties of Organic Layered Material by Intercalation. *Chem-Us* 2017, **3**(3)**:** 509-521.

35. Polacchi L, Brosseau A, Metivier R, Attain C. Mechano-responsive fluorescent polydiacetylene-based materials: towards quantification of shearing stress at the nanoscale. *Chem Commun* 2019, **55**(97)**:** 14566-14569.

36. Ortuso RD, Sugihara K. Detailed Study on the Failure of the Wedge Calibration Method at Nanonewton Setpoints for Friction Force Microscopy. *J Phys Chem C* 2018, **122**(21)**:** 11464-11474.

37. Ogletree DF, Carpick RW, Salmeron M. Calibration of frictional forces in atomic force microscopy. *Review of Scientific Instruments* 1996, **67**(9)**:** 3298-3306.

38. Varenberg M, Etsion I, Halperin G. An improved wedge calibration method for lateral force in atomic force microscopy. *Review of Scientific Instruments* 2003, **74**(7)**:** 3362-3367.

39. Alice A. Deckert JCH, Barry Valentine, Lisa Kiernan, and Lara Fallon. Effects of Molecular Area on the Polymerization and Thermochromism of Langmuir-Blodgett Films of Cd2+ Salts of 5,7-Diacetylenes Studied Using UV-Visible Spectroscopy. *Langmuir* 1995, **11**(2)**:** 643-649.

40. Nuck J, Sugihara K. Mechanism of Polydiacetylene Blue-to-Red Transformation Induced by Antimicrobial Peptides. *Macromolecules* 2020, **53**(15)**:** 6469-6475.

41. Terada H, Imai H, Oaki Y. Visualization and Quantitative Detection of Friction Force by Self-Organized Organic Layered Composites. *Adv Mater* 2018, **30**(27)**:** e1801121.

42. Kolusheva S, Shahal T, Jelinek R. Peptide-membrane interactions studied by a new phospholipid/polydiacetylene colorimetric vesicle assay. *Biochemistry* 2000, **39**(51)**:** 15851-15859.

43. Hankin SHW, Downey MJ, Sandman DJ. On the Structural Origins of Solid-State Urethane Polydiacetylene Thermochromism - Thermal and Structural-Properties of Ipudo Monomer and Polymer. *Polymer* 1992, **33**(23)**:** 5098-5101.

44. Lifshitz Y, Golan Y, Konovalov O, Berman A. Structural transitions in polydiacetylene Langmuir films. *Langmuir* 2009, **25**(8)**:** 4469-4477.

45. Wang H, Han SH, Hu YF, Qi ZM, Hu CS. Polydiacetylene-based periodic mesoporous organosilicas with colorimetric reversibility under multiple stimuli. *Colloid Surface A* 2017, **517:** 84-95.

46. van der Spoel D, van Maaren PJ, Larsson P, Timneanu N. Thermodynamics of hydrogen bonding in hydrophilic and hydrophobic media. *J Phys Chem B* 2006, **110**(9)**:** 4393-4398.

47. Markovitch O, Agmon N. Structure and energetics of the hydronium hydration shells. *J Phys Chem A* 2007, **111**(12)**:** 2253-2256.

48. Reynolds JA, Gilbert DB, Tanford C. Empirical Correlation between Hydrophobic Free-Energy and Aqueous Cavity Surface-Area. *P Natl Acad Sci USA* 1974, **71**(8)**:** 2925-2927.

49. Zhang H, Li X, Lin Y, Gao F, Tang Z, Su P, Zhang W, Xu Y, Weng W, Boulatov R. Multi-modal mechanophores based on cinnamate dimers. *Nat Commun* 2017, **8**(1)**:** 1147.

50. Carpick RW, Mayer TM, Sasaki DY, Burns AR. Spectroscopic ellipsometry and fluorescence study of thermochromism in an ultrathin poly(diacetylene) film: Reversibility and transition kinetics. *Langmuir* 2000, **16**(10)**:** 4639-4647.

51. Deckert AA, Fallon L, Kiernan L, Cashin C, Perrone A, Encalarde T. Kinetics of the Reversible Thermochromism in Langmuir-Blodgett-Films of Cd2+ Salts of Polydiacetylenes Studied Using Uv-Vis Spectroscopy. *Langmuir* 1994, **10**(6)**:** 1948-1954.

52. Diesendruck CE, Peterson GI, Kulik HJ, Kaitz JA, Mar BD, May PA, White SR, Martinez TJ, Boydston AJ, Moore JS. Mechanically triggered heterolytic unzipping of a low-ceiling-temperature polymer. *Nat Chem* 2014, **6**(7)**:** 623-628.

53. Sagara Y, Karman M, Verde-Sesto E, Matsuo K, Kim Y, Tamaoki N, Weder C. Rotaxanes as Mechanochromic Fluorescent Force Transducers in Polymers. *J Am Chem Soc* 2018, **140**(5)**:** 1584-1587.

Graphic TOC